Phase tracking using a geometrical approach : theory and application on FMCW radar.

Massimo D'ELIA Mykhailo ZARUDNIEV Stephane BONNET
University Grenoble Alpes, CEA, LETI, Minatec, F-38000, Grenoble, France

Résumé – L'estimation des variations de phase d'un signal sinusoidal peut être menée dans le domaine de Fourier. Le papier propose d'étudier une approche géométrique en démontrant que la bin fréquentielle décrit une ellipse dans le plan complexe. On améliore ainsi le suivi de phase et l'estimation des déplacements sub-millimetriques en prenant en compte cet aspect ; ce résultat est démontré sur des données fournies par un radar millimétrique.

Abstract – Estimating the phase variation of a sinusoidal signal can be performed in the Fourier domain. This paper proposes to investigate a geometrical viewpoint and demonstrate that the frequency bin of interest is distributed along an ellipse in the complex plane. One can improve phase tracking at least theoretically by accounting for this observation and improve the sub-millimeter displacement estimation. This result is demonstrated on data provided by a millimeter-wave radar.

1 Introduction

The Discrete Fourier Transform (DFT) is a powerful tool to investigate the frequency content of a signal. Furthermore, in several applications, the estimation and the time evaluation of the signal phase is fundamental. Among these, the radar applications are of growing interest, due to recent improved integration and cost. Interesting applications vary from the automotive to the healthcare field : while in the former their implementation can be considered established [7], in the latter first commercial applications are increasingly appearing [4]. In these cases, the target displacement is estimated from the beat signal phase. If this estimation is done through a DFT approach, it is generally assumed that the complex components of the corresponding frequency bin should describe, in their time evolution, a circle of unity radius and centered in the complex plane origin. We show in this work that this is generally not the case : the trajectory is inherently ellipse shaped. This translates into a phase (and therefore displacement) estimation error : this error can be up to $\approx 1.6\%$ the carrier wavelength and can be significative for submillimetric displacements. In Section 2, we show the DFT transform of a pure tone signal and how the complex components evolution describe an ellipse shape, under certain conditions. In section 3, we briefly sum up the lossless model of a FMCW signal and the related interest for a DFT approach. Then, in Section 4, we compare the theoretical curve with actual radar measurements.

2 A theoretical DFT study

Consider the N-point sinusoidal signal with amplitude M, normalized frequency α and initial phase angle ϕ [rad]

$$s_n = M\cos\left(\alpha n + \phi\right), \quad n = 0, \ldots, N-1 \tag{1}$$

where the normalized frequency can be defined as

$$\alpha = 2\pi\frac{f}{f_s} = 2\pi\frac{p}{N} \tag{2}$$

and f_s the sampling frequency [Hz].
In this work, we are interested in deriving an analytical formula for the k-th DFT bin :

$$S_k = \frac{1}{N}\sum_{n=0}^{N-1} s_n e^{-i\beta_k n}, \quad k = 0, \ldots, N-1 \tag{3}$$

where $i = \sqrt{-1}$ and $\beta_k = 2\pi\frac{k}{N}$. The discrepancy between the true frequency and the DFT frequency is denoted $\delta = \alpha - \beta_k = (p-k)2\pi/N$.

For the signal under test, we have

$$S_k = \frac{M}{2N}\left[e^{i\phi}\sum_{n=0}^{N-1} e^{i(\alpha-\beta_k)n} + e^{-i\phi}\sum_{n=0}^{N-1} e^{i(\alpha+\beta_k)n}\right] \tag{4}$$

p integer It is a simple matter to show that $S_p = S_{N-p} = M/2e^{i\phi}$ and $S_k = 0$ otherwise. In this case, all the signal energy is concentrated in one bin.

p not integer Using geometric series, we obtain [2]

$$\begin{aligned} S_k &= \frac{M}{2N}\left[e^{i\phi}\cdot\frac{1-e^{i(\alpha-\beta_k)N}}{1-e^{i(\alpha-\beta_k)}} + e^{-i\phi}\cdot\frac{1-e^{-i(\alpha+\beta_k)N}}{1-e^{-i(\alpha+\beta_k)}}\right] \\ &= \frac{M}{2N}\left[\frac{Ue^{i\beta_k}-V}{\cos\alpha-\cos\beta_k}\right] \end{aligned}$$

where $U = \cos(\alpha N+\phi) - \cos\phi = M^{-1}(s_N - s_0)$ and $V = \cos(\alpha N+\phi-\alpha) - \cos(\phi-\alpha) = M^{-1}(s_{N-1} - s_{-1})$. Rearranging terms as $U = -2\sin(\alpha N/2+\phi)\sin(\alpha N/2)$ and $V = -2\sin(\alpha\,(N/2-1)+\phi)\sin(\alpha N/2)$, the DFT bin can be simplified into

$$S_k = a_k\left[\sin(\alpha N/2+\phi)e^{i\beta_k} - \sin(\alpha\,(N/2-1)+\phi)\right]$$

where

$$a_k = \frac{-M\sin(\alpha N/2)}{N(\cos\alpha-\cos\beta_k)},\ \alpha_0 = \frac{(N-1)}{2}\alpha$$

Applying a rotation of angle $\beta_k/2$ we obtain

$$\begin{aligned} e^{-i\beta_k/2}S_k &= 2a_k\cos(\beta_k/2)\sin(\alpha/2)\cos(\alpha_0+\phi) \\ &+ i\cdot 2a_k\sin(\beta_k/2)\cos(\alpha/2)\sin(\alpha_0+\phi) \end{aligned}$$

Splitting real and imaginary components $S_k = x_k + iy_k$ yields

$$\mathbf{R}\begin{pmatrix} x_k \\ y_k \end{pmatrix} = \mathbf{D}\begin{bmatrix} \cos(\alpha_0+\phi) \\ \sin(\alpha_0+\phi) \end{bmatrix} \tag{5}$$

with the rotation matrix

$$\mathbf{R} = \begin{bmatrix} \cos(\beta_k/2) & +\sin(\beta_k/2) \\ -\sin(\beta_k/2) & \cos(\beta_k/2) \end{bmatrix}$$

$$\mathbf{D} = 2a_k\begin{bmatrix} \cos(\beta_k/2)\sin(\alpha/2) & 0 \\ 0 & \sin(\beta_k/2)\cos(\alpha/2) \end{bmatrix}$$

Finally we obtain the main result of the paper

$$\boxed{\mathbf{z}_k = \begin{pmatrix} x_k \\ y_k \end{pmatrix} = \mathbf{R}^T\mathbf{D}\begin{bmatrix} \cos(\alpha_0+\phi) \\ \sin(\alpha_0+\phi) \end{bmatrix}} \tag{6}$$

It holds $\mathbf{z}_k^T\mathbf{A}\mathbf{z}_k = 1$ where $\mathbf{A} = \mathbf{R}^T\mathbf{D}^{-2}\mathbf{R}$ is symmetric positive definite (SPD). This indicates that the locus of each DFT bin is a **2-D ellipse** when ϕ varies. The inclination of the ellipse is controlled by β_k via the rotation matrix while the length of each ellipse axis is controlled by the matrix $\mathbf{D}$.
In the limit, the term a_k writes [2]

$$a_k = \frac{M}{2N}\frac{(-1)^k\sin\left(\frac{\delta N}{2}\right)}{\sin\left(\frac{\delta}{2}+\beta_k\right)\sin\left(\frac{\delta}{2}\right)} \underset{\delta\to 0}{\to} \frac{M}{2}\frac{(-1)^k}{\sin\beta_k}$$

and

$$\mathbf{D} \underset{\delta\to 0}{\to} 2a_k\cos(\beta_k/2)\sin(\beta_k/2)\mathbf{I}_2 = (-1)^k\frac{M}{2}\mathbf{I}_2$$

where $\mathbf{I}_2$ is the 2-by-2 identity matrix. This means that when the DFT bin is 'close' to the true frequency, the ellipse becomes a circle as expected. For the case where $k = p$, then

$$\mathbf{z}_p = \frac{M}{2}\begin{pmatrix} \cos\phi \\ \sin\phi \end{pmatrix}$$

and in this case the DFT bin belongs to a 2-D circle.

When there exists a DFT bin such that $\beta_k \simeq \alpha$, we see that the eccentricity of the ellipse will be small (i.e. the ellipse tends to a circle) and the diagonal matrix is a multiple of $\mathbf{I}_2$. This is shown in Figure 1, where the blue curve represents Eq. (6) for $p = 2.5$, $k = 2$ and $M = 3$. The red curve represents the circle of radius $M/2$ which we would obtain if $p = k$. In this case, the rotation angle is $\beta_k/2 \approx 3.6\,\text{deg}$ while the major and minor axes are 1.06 and 0.85, respectively.

It must also be noted that, in order to correctly estimate the phase angle ϕ, we need to correct the elliptical shape of $\mathbf{z}_k$. We then calculate $\mathbf{z}_{k,corr}$ as

$$\mathbf{z}_{k,corr} = \mathbf{R}\mathbf{D}^{-1}\mathbf{z}_k \tag{7}$$

from which we estimate the corresponding phase as

$$\hat{\phi} = \arctan\left(\frac{\mathbf{z}_{k,corr.2}}{\mathbf{z}_{k,corr.1}}\right) \tag{8}$$

where the $1, 2$ indexes indicates the vector component along the first and second direction along an orthonormal basis. A last remark is about how the correction method could be applied. When experimental data is available, a shape fitting algorithm could be applied to the dataset and the ellipse parameters are then retrieved. In this case, the matrices $\mathbf{R}$ and $\mathbf{D}$ are directly estimated. Another approach would be to estimate *a priori* the a_k value. This could be done like in [1]. Then, both $\mathbf{R}$ and $\mathbf{D}$ can be calculated and the correction procedure carried out.

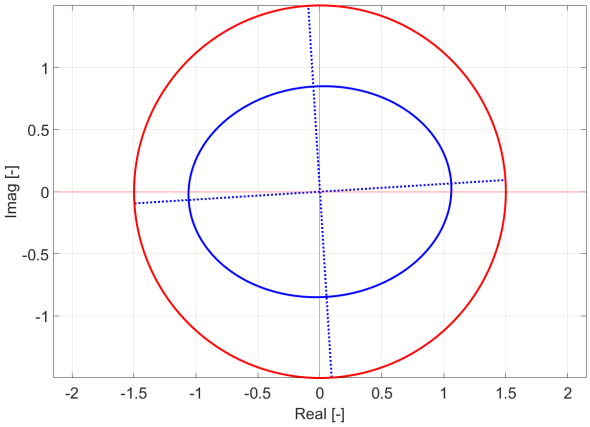

FIGURE 1 : DFT bin locus for the case of $p = k$ (red curve) and $p = 2.5$, $k = 2$ (blue curve). For both cases a magnitude of M=3 is imposed.

3 FMCW Radar Data and Motion Detection Scheme

In a FMCW radar system, the transmitted signal is frequency-modulated and can be written as :

$$s_{TX}(t) = \sqrt{A}\cos\left(\varphi_0 + 2\pi\left[f_0 t + \frac{1}{2}\gamma t^2\right]\right), \quad t \in [0, T_c] \tag{9}$$

where f_0 is the chirp initial frequency (Hz). The bandwidth of the signal is Δf (Hz), T_c is the chirp time duration (s) and $\gamma = \Delta f/T_c$ (Hz s^{-1}) is the chirp frequency slope.
The received (lossless) reflected signal can be written as

$$s_{RX}(t) = s_{TX}(t-\tau) \tag{10}$$

where $\tau = 2R/c$ is the round-trip time delay (s) for a single target located at a distance R and c is the speed of light.
At reception, both transmitted and reflected signals are mixed and Low-Pass (LP) filtered, in order to produce the so-called Intermediate Frequency (IF) signal s_{IF}

$$\begin{aligned} s_{IF}(t) &= LP\{s_{TX}(t)\cdot s_{RX}(t)\} \\ &= \frac{A}{2}\cos\left[2\pi\tau\left(f_0+\gamma t-\frac{\gamma\tau^2}{2}t\right)\right] \quad (11) \\ &\approx \frac{A}{2}\cos\left[2\pi\tau\left(f_0+\gamma t\right)\right] \quad (12) \end{aligned}$$

The approximation is justified by the measuring distances which are usually considered for FMCW applications. For a target at 3 m distance, $\tau = 20\cdot 10^{-9}$s while a high performance value of γ would be $\approx 4\cdot 10^{13}$ GHz $\cdot\,\text{s}^{-1}$. Then, $\gamma\tau^2 \approx 0.016$ and therefore Eq. 12 can be considered valid.

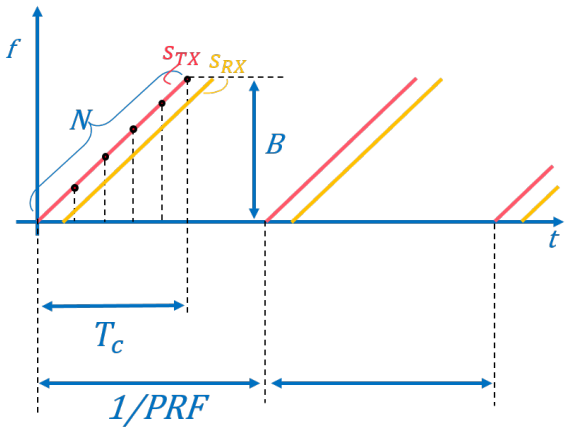

FIGURE 2 : The transmitted chirps will have a repetition period of $1/PRF$ (slow time) while received chirps will have a delay (τ) linked to the distance of the target.

In this ideal situation, which can be thought to be approximately attained in good Signal-to-Noise Ratio (SNR) conditions, s_{IF} is a sinusoidal signal with frequency $f_{IF} = \gamma\tau$. It is important to note that both frequency and phase of the IF signal depend on the target distance R via their dependency in τ.

Small Movements In the scenario of a *small* movement around the position $\bar{R}$, the beat frequency will change by $\Delta f = 2\pi\Delta R/c \cdot \gamma$ while its phase changes by a the amount $\Delta\varphi = 4\pi\Delta R/c \cdot f_0$ (see Eq. 12). Assuming the same case parameters as before plus $f_0 = 122$ GHz, we can see that a $\Delta R = .2$ mm displacement would give

$$\begin{cases} \Delta f = 167.55 \text{ Hz } (f_{IF} = 2.51 \text{ MHz}) \\ \Delta\varphi = 1.02 \text{ rad} \end{cases} \tag{13}$$

Then, we can assume that the beat frequency remains constant for sub-millimetric movements. This means that the target bin dos not change as well. On the other hand, the phase will change proportionally to the target displacement ΔR.
Once the frequency f_{IF} is estimated, the target distance can be obtained from

$$\bar{R} = \frac{c}{2\gamma} f_{IF} \tag{14}$$

with a spatial resolution of $c/2B$. Spatial resolution from Eq. (14) is limited by the available bandwidth and therefore cannot deliver sub-millimetric resolution. From Eq. (12), we can see that also the signal phase is linked to the target distance by

$$\varphi_{IF}(R) = 2\pi f_0 \tau = 4\pi R/\lambda_0 \tag{15}$$

where $\lambda_0 = c/f_0$. Since phase information is limited in the $[0, 2\pi]$ interval, no absolute distance can be estimated from this information. However, as chirps are emitted at a given Pulse Repetition Frequency (PRF), it is possible to track the target displacement around the mean distance $\bar{R}$ whether the corresponding signal frequency (i.e. the frequency bin) is unchanged. Therefore, the PRF will determine the radar system time resolution. We can estimate the target displacement as

$$\Delta R = \frac{\Delta\varphi_{IF}}{2\pi} \frac{\lambda_0}{2} \tag{16}$$

i.e. the sub-millimetric spatial resolution is linked to the central wavelength λ_0.

4 Results

As shown above, in order to estimate the sub-millimetric displacement of a target by the means of a FMCW radar system, we apply Eq. (16) from the estimated phase of the IF signal. Specifically, this must be done along consecutive chirps (which is the so called *slow* time). We can estimate this phase through a DFT approach by following the phase evolution of the k-th bin along the slow time. This would mean applying Eq. (3) to Eq. (12), to which the considerations from Section 2 apply. Realistically, the corresponding frequency $f_{DFT} = 2\pi k/N$ of the k-th bin will be close but not equal to the angular frequency α. Furthermore, the value of α will not be known a priori (not at least from a radar measurement). This means that the complex locus of the complex radar (DFT transformed) signal will be an ellipse. It can be interesting then to evaluate the intrinsic error which is introduced when the DFT is adopted for phase estimation. This error is basically due to the fact that we directly retrieve the phase from an elliptic complex locus. In Figure 3-a this error is shown for a constant δ difference ($\delta = 0.3$) and different values of p and k. Specifically, the error between the expected angle ϕ and the relative angle $\phi_e - \phi_{e,0}$ is shown. We can appreciate how the error magnitude is larger for smaller values of k, while it has a maximum around $\pi/4$ (for δ=0.5). The former is due to the fact that the ellipse eccentricity is inversely proportional to the value of k. The latter is linked to the δ chosen value, as can be appreciated from Figure 3-b where the error as a function of δ is shown. Also in this case, when the difference δ increases, the eccentricity increases, thus producing a larger error. We can also observe that the position of this maximum changes with δ, which depends on the non-linear and trigonometric nature of $\partial(\hat{\phi} - \phi)/\partial\delta$.

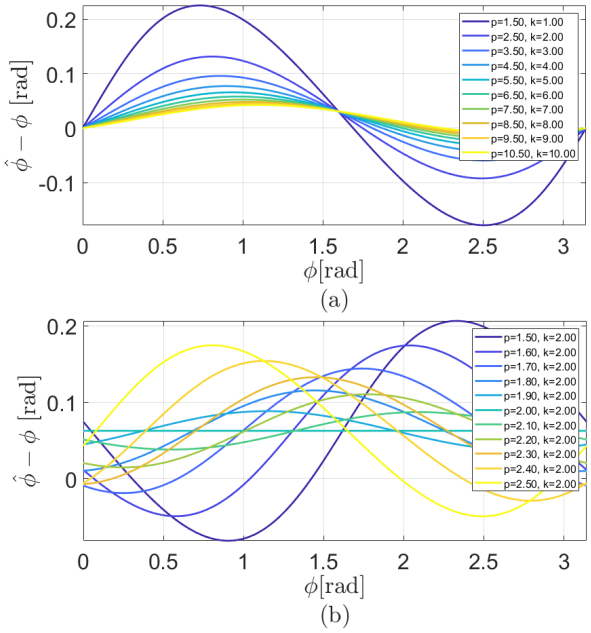

FIGURE 3 : Phase estimation error for (a) a fixed δ value and (b) a varying δ value, for a fixed k-th bin

It is interesting to notice that, whenever $p \notin N$, the phase information is present in all frequency bins. This information is affected by the error shown in Fig. 3 which, however, can be alleviated if a compensation of the elliptic distortion is applied. This is shown in Fig. 4-c, where the DFT for an integer and rational p ($p = 2, k = 2$ and $p = 2.2, k = 2$, resp.) are shown. In Fig. 4-a, the corresponding error at the three indicated frequency bins are shown. These errors are exclusively due to the elliptic shape of z_k. In Fig. 4-b, the same error is calculated after compensation as per Eq. 7.

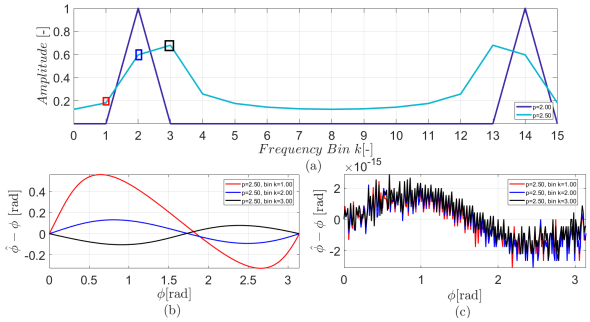

FIGURE 4 : DFT of a pure sine for (a) an integer and rational value of p. In (b) errors corresponding to the frequency bins $k = 1 \ldots 3$ (red, blue and black lines, respectively). In (c) errors after ellipse compensation for the same frequency bins.

4.1 Radar Data

In this section, we show radar data from real experimental acquisitions. The radar system considered is the commercial solution SiRad SIMPLE manufactured by Silicon Radar, while the target was a cylindrical target of 6 mm diameter screwed on a linear actuator who could make very precise displacements (< 3 μm accuracy) up to 25 mm. The target was displaced of 8 mm from the idle position, in order to cover at least a full $[0, 2\pi]$ angular interval in the corresponding DFT complex plane. The target was put at a distance of 0.282 m from the radar, while the radar measurement of this distance was estimated to be 0.276, which corresponds to the 7th DFT bin ($k = 7$). The discrepancy between p and k will give rise to a theoretical elliptic curve in the complex plane. Therefore, we show in Figure 5 the radar measurement scatter plot with the ellipse obtained from Eq. (6). Here the magnitude value M was fitted. We can see that data is scattered along an ellipse whose parameters estimated by Eq. (6) are :

$$p = 7.15, \; k = 7 \tag{17}$$

$$\beta_k = 1.67, \; a = 151.87, \; b = 155.22 \tag{18}$$

where a and b are the minor and major axes of the ellipse.

5 Conclusions

In the present work, we investigated the theoretical form of a DFT of a pure real sinusoidal signal. Specifically, we are interested in the case where the frequency bin does not necessarily match the normalized frequency of the analyzed signal. This is what would usually happen in (among many applications)

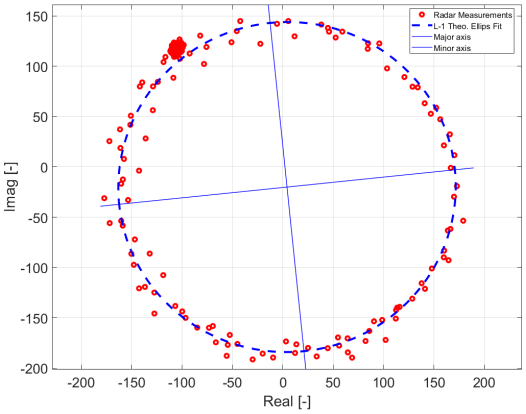

FIGURE 5 : DFT of radar measurements (red circles) of a 8 mm displacement movement. The blue dashed line represents the theoretical DFT ellipse fitted in magnitude, while the two blue thin lines represent its orientation

FMCW systems, if a DFT approach was chosen to analyze the output IF signal. We showed that the DFT complex components will describe an ellipse in the complex plane. Therefore, even in ideal conditions, an error will be introduced in the phase retrieval of such a signal. This error is linked to the deformation due to the ellipse shape and, therefore, will be strongly linked to the difference between the frequency bin and signal frequency (i.e. the value of δ) but also to the absolute value of k. Finally, we showed that this theoretical curve is retrieved in radar data from an experimental measurement. Therefore, if a phase estimation should be made starting from a DFT transformed signal, a compensation for such an elliptical shape of the complex components should be made.

Références

[1] C CANDAN : Fine resolution frequency estimation from three dft samples : Case of windowed data. *Signal Process.*, 114:245–250, 2015.

[2] W. CEDRON : DFT bin value formulas for pure real tones. *DSPRelated.com*, 2015.

[3] T. DAI et al. : Enhancement of remote vital sign monitoring detection accuracy using multiple-input multiple-output 77 GHz FMCW radar. *IEEE J. Electromagn. RF Microw. Med. Biol.*, 6(1):111–122, 2022.

[4] Y. LEE et al. : A novel non-contact heart rate monitor using impulse-radio ultra-wideband (IR-UWB) radar technology. 08 2018.

[5] C. LI et al. : A review on recent progress of portable short-range noncontact microwave radar systems. *IEEE Trans. Microw. Theory Techn.*, 65(5):1692–1706, 2017.

[6] J. LIU et al. : Accurate measurement of human vital signs with linear FMCW radars under proximity stationary clutters. *IEEE T. Biomed. Circ. S.*, 15(6):1393–1404, 2021.

[7] S. M. PATOLE et al. : Automotive radars : A review of signal processing techniques. *IEEE Signal Process. Mag.*, 34(2):22–35, 2017.